



저작자표시-비영리-변경금지 2.0 대한민국

이용자는 아래의 조건을 따르는 경우에 한하여 자유롭게

- 이 저작물을 복제, 배포, 전송, 전시, 공연 및 방송할 수 있습니다.

다음과 같은 조건을 따라야 합니다:



저작자표시. 귀하는 원저작자를 표시하여야 합니다.



비영리. 귀하는 이 저작물을 영리 목적으로 이용할 수 없습니다.



변경금지. 귀하는 이 저작물을 개작, 변형 또는 가공할 수 없습니다.

- 귀하는, 이 저작물의 재이용이나 배포의 경우, 이 저작물에 적용된 이용허락조건을 명확하게 나타내어야 합니다.
- 저작권자로부터 별도의 허가를 받으면 이러한 조건들은 적용되지 않습니다.

저작권법에 따른 이용자의 권리는 위의 내용에 의하여 영향을 받지 않습니다.

이것은 [이용허락규약\(Legal Code\)](#)을 이해하기 쉽게 요약한 것입니다.

[Disclaimer](#)

수의학석사학위논문

Induction of Th2-related mucosal immunity by intranasal immunization of *Brucella abortus* malate dehydrogenase loaded chitosan nanoparticles

Brucella abortus malate dehydrogenase가 담지 된 키토산 나노 입자의 비강 면역에 의한 Th2 관련 점막 면역 유도

2019 年 2 月

서울대학교 대학원

수의학과

수의병인생물학 및 예방수의학 전공

소 상 회

**Induction of Th2-related mucosal immunity by intranasal
immunization of *Brucella abortus* malate dehydrogenase
loaded chitosan nanoparticles**

By

Sang Hee Soh

February, 2019

**Department of Veterinary Medicine
(Major : Veterinary Pathobiology and Preventive medicine)
The Graduate School
Seoul National University**

**Induction of Th2-related mucosal immunity by intranasal
immunization of *Brucella abortus* malate dehydrogenase
loaded chitosan nanoparticles**

A Dissertation

**Submitted to the Graduate School in Partial Fulfillment of the
Requirements for the Degree of Master**

**To the Faculty of College of Veterinary Medicine
Department of Veterinary Medicine
The Graduate School
Seoul National University**

By

Sang Hee Soh

2018

**Induction of Th2-related mucosal immunity by intranasal
immunization of *Brucella abortus* malate dehydrogenase
loaded chitosan nanoparticles**

지도교수 : 유 한 상

이 논문을 수의학석사 학위논문으로 제출함
2018 년 12 월

서울대학교 대학원
수의학과
수의병인생물학 및 예방수의학 전공
소 상 희

소상희의 수의학석사 학위논문을 인준함
2018 년 12 월

위 원 장 _____ 권 혁 준 (인)

부위원장 _____ 유 한 상 (인)

위 원 _____ 허 은 미 (인)

Abstract

Induction of Th2-related mucosal immunity by intranasal immunization of *Brucella abortus* malate dehydrogenase loaded chitosan nanoparticles

Sang Hee Soh

(Supervisor: Han Sang Yoo, D.V.M., Ph.D)

Department of Veterinary Medicine
The Graduate School
Seoul National University

The aim of this study was to investigate the induction of mucosal immune responses by intranasal immunization of an important *Brucella abortus* antigen, malate dehydrogenase (Mdh), loaded in mucoadhesive chitosan nanoparticles (CNs) in a BALB/c mouse model. The production of cytokines was investigated in human leukemic monocyte cells (THP-1 cells) after stimulation with the nanoparticles. Mdh-loaded CNs (CNs-Mdh) induced higher interleukin (IL)-6 production than unloaded antigens and trigger factor (TF) loaded CNs (CNs-TF). Using ELISpot to quantify

cytokines and antibody-secreting cells in the intranasally immunized mice, IL-4 and IgG-secreting cells were found to be significantly increased at 4 weeks and 6 weeks post-immunization in the CNs-Mdh immunized group, respectively. Increases in Mdh-specific IgG, IgG1, and IgG2a antibodies were confirmed at 6 weeks after immunization, indicating a predominant IgG1 response. Analysis of the mucosal immune response in the intranasally immunized mice revealed that Mdh-specific and total IgA in the nasal washes, genital secretions, fecal extracts and sera were remarkably increased in the CNs-Mdh-immunized group compared to the CNs-TF-immunized group except total IgA of nasal washes. Therefore, the results indicated that the intranasal immunization of CNs-loaded *B.abortus* Mdh antigen effectively induced antigen-specific mucosal immune responses through the elicitation of Th2-related immune responses.

Keywords: *Brucella abortus*, malate dehydrogenase, chitosan nanoparticles, Th2 immune response, mucosal immune response

Student Number: 2017-29538

Contents

Abstract	i
Contents	iii
List of figures	iv
List of tables	vi
List of abbreviations	vii
1. Introduction	1
2. Materials and Methods	4
2.1. Purification of <i>B. abortus</i> malate dehydrogenase	4
2.2. Preparation of chitosan nanoparticles	5
2.3. Loading of recombinant proteins	5
2.4. Characterization of chitosan nanoparticles	6
2.5. <i>In vitro</i> studies	6
2.5.1. Release test	6
2.5.2. Immunocytochemistry in THP-1 cells	6
2.5.3. Measurement of secreted cytokines in THP-1 cells	7
2.6. <i>In vivo</i> studies	8
2.6.1. Intranasal immunization of mice	8
2.6.2. ELISpot assays for total IgG, IFN- γ and IL-4	9
2.6.3. Measurement of antibody production	10
2.7. Statistical analysis	11
3. Results	12
3.1. SDS-PAGE and Western blotting	12
3.2. Characterization of recombinant protein-loaded CNs	14
3.3 <i>In vitro</i> studies	16
3.3.1. Loading efficacy measurements and release tests for the protein-loaded CNs	16
3.3.2. Immunocytochemistry in THP-1 cells	19
3.3.3. Cytokine measurement in stimulated THP-1 cells	21
3.4 <i>In vivo</i> studies	23
3.4.1. ELISpot	23
3.4.2. Measurement of Mdh specific antibodies	25
3.4.3. Measurement of total IgA	27
4. Discussion	29
5. Conclusion	33
6. References	34
7. 국문초록	40

List of figures

- Figure 1 (A) SDS-PAGE profiles indicated purified proteins. (B) Western blotting of the recombinant proteins expressed from the pCold TF vector were confirmed using an anti-histidine antibody.
- Figure 2 (A) SEM photographs of the CNs, CNs-TF and CNs-Mdh and (B) the average particle size distribution of the CNs, CNs-TF and CNs-Mdh using dynamic light scattering.
- Figure 3 Release of TF and Mdh from loaded chitosan nanoparticles.
- Figure 4 Confocal microscopic analysis after immunofluorescence staining showing the nuclear localization of anti-his tag antibody conjugated with Alexa Fluor 488 (green) and nuclear staining with DAPI (blue). (A) Confocal images taken at 2 h, 6 h, and 12 h after stimulation with Mdh alone in THP-1 cells. (B) Confocal images taken at 2 h, 6 h, and 12 h after stimulation with CNs-Mdh in THP-1 cells.
- Figure 5 TNF- α (A) and IL-6 (B) concentrations in the supernatants of THP-1 cells at 6 h, 12 h and 24 h after primary stimulation. Cells (1×10^6 cells/well) were stimulated with 10 μ g of each antigen.
- Figure 6 ELISpot analysis in immunized mouse splenocytes. (A) The numbers of IgG, IL-4 and IFN- γ -secreting cells are shown at 4 weeks after primary immunization. (B) The numbers of IgG, IL-4 and IFN- γ -secreting cells per 2.5×10^5 cells are shown at 6 weeks after primary immunization.
- Figure 7 Mdh-specific antibody measurements at 6 weeks after primary intranasal immunization. (A) Mdh specific total IgG, (B) IgG1 and

(C) IgG2a in the sera of immunized mice. Secreted IgA and serum IgA were measured in mucosal samples and sera. Significant increase in the IgA levels of (D) nasal washes, (E) genital secretions, (F) fecal extracts and (G) sera were observed between the CNs-TF and CNs-Mdh-immunized groups.

Figure 8 Total IgA measurements in the nasal wash, genital secretion, fecal extract and serum samples at each time point (2, 4 and 6 weeks after primary immunization).

List of tables

Table 1 Loading efficiency of TF and Mdh in chitosan nanoparticles

List of abbreviations

ASCs	Antigen-secreting cells
CNs	Chitosan nanoparticles
CNs-Mdh	Malate dehydrogenase-loaded chitosan nanoparticles
CNs-TF	Trigger factor-loaded chitosan nanoparticles
DLS	Dynamic light scattering
ELISA	Enzyme-linked immunosorbent assay
ELISpot	Enzyme-linked immunosorbent spot
IFN-γ	Interferon-gamma
IgA	Immunoglobulin A
IgG	Immunoglobulin G
IL	Interleukin
Mdh	Malate dehydrogenase
SEM	Scanning electron microscopy
TCA	Tricarboxylic acid
TF	Trigger factor
THP-1	Human leukemic monocyte cells
TLR	Toll-like receptor
TNF-α	Tumor necrosis factor-alpha
TPP	Triphosphate

1. Introduction

Brucellosis is a globally widespread zoonotic disease that is transmitted from domestic animals to humans, either directly or indirectly through contact with infected animals or animal products. *Brucella* is classified into eleven species according to host specificity, and four species infect humans [1, 2]. Of these, *B. abortus* is a causative organism of bovine brucellosis and can be a major threat to human health due to its high infectivity. The transmission of brucellosis to humans occurs through a variety of routes including the ingestion of unpasteurized animal-dairy products, direct contact with infected animal parts, and inhalation of infected aerosolized particles [3]. In this regard, focusing on stopping the spread of disease through the use of effective and safe vaccines to prevent and control both human and bovine brucellosis is important.

Strains 19 and RB51 are the *B. abortus* vaccine strains most commonly used to protect cattle against infection and abortion [4]. However, as these vaccines have several disadvantages, much effort has been devoted to developing a safe and effective subunit vaccine with recombinant proteins [5-9]. Therefore, cattles and mice were experimentally infected with *B. abortus* strains in order to find reliable antigenic proteins as vaccine candidates and analyzed proteomic identification by two-dimensional electrophoresis and western blotting with antiserum [10, 11]. After excluding several cross-reactive spots, immunodominant proteins that showed strong immunoblots during observation period were selected [10, 11]. Through *in vitro* and *in vivo* experiments with several purified immunodominant proteins, Mdh with high potential as a vaccine candidate

protein was selected. Malate dehydrogenase (Mdh), a key enzyme in the tricarboxylic acid (TCA) cycle, elicited high cytokine production and toll-like receptor (TLR) expression in human leukemic monocyte cells (THP-1) cells that were stimulated by several recombinant proteins [12]. In addition, vaccination via the intraperitoneal injection of purified *B. abortus* Mdh was reported to significantly reduce colonization and cause the rapid elimination of S19 in BALB/c mice [13]. However, traditional vaccination strategies, which require multiple injections using needles or other invasive routes, have problems with administration, needle cross-contamination, cost and patient compliance [14]. In this regard, mucosal immunization using recombinant proteins is a very attractive vaccine choice because of its safety and effective induction of immunity through natural routes without needles.

The mucosal surface serves as the first line of defense against infection as it is the initial contact site for pathogens [15]. The induction of secretory IgA from the mucosa blocks bacterial and viral adhesion to the mucosal surface and prevents damage to the host. The mucosal immune response is most effective when a vaccine is administered to the mucosal surface; however, injection vaccines do not always reach mucosal surfaces and are consequently less effective at preventing mucosal surface infections [16]. In particular, the intranasal route shows relatively less proteolytic activity, which can protect protein antigens from enzymatic degradation, thus requiring fewer antigens than the oral route [17]. Additionally, the nasal epithelium is highly permeable and vascularized with cervical lymph nodes and lymphoid cells [17]. Therefore, antigens are easily accessible if they can be transported properly through the epithelium. However, despite these beneficial features, one of the most important limitations of nasal immunity is the rapid mucociliary clearance that occurs at the mucosal surface, which

hinders antigen delivery because the immunogen formulation is rapidly removed from the mucosa. Materials administered through the nasal cavity have been reported to be removed from the nasal membranes within approximately 21 min via mucociliary clearance [18]. Therefore, increasing the residence time of antigens in the nasal cavity to increase their contact time with the nasal mucosa to induce effective nasal mucosal immunity is necessary.

Effective adjuvants are needed for antigen delivery systems because recombinant protein antigens delivered to mucosa are often not highly immunogenic. Recently, chitosan has been attracting attention as a promising polymer due to its nontoxic, biocompatible, and biodegradable nature, as well as its mucoadhesive and permeation-enhancing properties [19, 20]. Nanoparticles or microspheres are very common forms used in controlled vaccine and drug delivery formulations. A spherical form is known to increase the residence time of vaccines on the mucosal surface compared to solutions because the sphere absorbs water from mucus and dehydrates the epithelial cells to separate the tight junctions [21]. The chitosan nanoparticles (CNs) used in this study are the most widely studied drug delivery system for the controlled release of antibiotics, antihypertensive agents, proteins, peptide drugs, and vaccines [22-24]. Previous studies have shown that CNs enhance mucosal absorption and have adjuvant activity in the mucosal immune response through intranasal administration [19, 25].

In the present study, CNs were prepared and characterized as an adjuvant for the controlled release of *B. abortus* Mdh. The immuno-stimulating activity of Mdh-loaded CNs (CNs-Mdh) was measured by examining the systemic and local mucosal immune responses that were elicited through

intranasal immunization in mice.

2. Materials and Methods

2.1. Purification of *B. abortus* malate dehydrogenase

The bacterial strains were the same as those used in a previous study [12]. The amplified Mdh DNA product was cloned into a pCold TF vector (Takara, Japan), transformed into *E. coli* DH5 α competent cells. Each *E. coli* DH5 α clones containing a recombinant plasmid was grown in Luria Bertani (LB, Difco) agar supplemented with ampicillin (Duchefa Biochemie, 100 μ g/ml). A single colony was inoculated into 60 ml of LB broth (100 μ g/ml ampicillin), which was then incubated at 37 °C overnight with agitation at 220 rpm. Sixty milliliters of each culture were inoculated into 1 L of terrific broth containing 100 μ g/ml ampicillin and grown under the same conditions to an OD₆₀₀ of 1.5. Cells were induced with 1 mM isopropyl β -D-1-thiogalactopyranoside (IPTG; Amresco, USA), and incubation was continued with shaking at 15 °C for 12 h. The bacterial cell pellets were then harvested and resuspended in binding buffer (20 mM Tris–HCl, 8 M urea, 500 mM NaCl, 20 mM imidazole [pH 8.0], and 1 mM β -mercaptoethanol (Sigma, USA). Each bacterial suspension was sonicated on ice, and the supernatants were collected after centrifugation at 3,000 \times g for 20 min. The recombinant proteins were purified under denaturing conditions using a His SpinTrap (GE Healthcare, UK) according to the manufacturer's protocol. Protein concentration was determined via Pierce 660 nm protein assays (Thermo Scientific, USA). The recombinant proteins were analyzed by SDS-PAGE and Western blotting with a 6x-His Tag Monoclonal Antibody (Thermo Scientific, USA).

2.2. Preparation of chitosan nanoparticles

Chitosan nanoparticles were prepared based on the ionic gelation of chitosan with sodium tripolyphosphate (TPP) anions. Water-soluble chitosan provided by Jakwang (deacetylation degree of 82.4%, Ansong, Korea) was dissolved in distilled water (0.5 wt.-%), and 300 μ l of an 8% Tween-80 solution was added to 50 ml of the chitosan solution. Using a 26G needle, 500 μ l of an aqueous TPP solution (10 wt.-%) was added dropwise into 50 ml of the water-soluble chitosan solution (0.5 wt.-%) containing Tween-80 under magnetic stirring and sonication (6 W, 10 min) on ice. Chitosan nanoparticles were obtained by centrifugation at 2,169 \times g for 20 min and were freeze-dried after being rinsed with distilled water.

2.3. Loading of recombinant proteins

Twenty milligrams of chitosan nanoparticles were dispersed in 1 ml of protein solution (4 mg/ml, pH 7.4 PBS). The suspension was kept at 37 $^{\circ}$ C for 24 h with continuous shaking, followed by centrifugation at 708 \times g for 10 min to remove unloaded proteins. The loading efficiency was measured by quantifying the unloaded protein in the supernatant via Pierce 660 nm protein assays kit. The loading efficiency (%) was calculated using following equation.

$$\text{Loading efficiency (\%)} = \frac{\text{Total amount of protein-unloaded protein}}{\text{Total amount of protein}} \times 100$$

2.4. Characterization of chitosan nanoparticles

The particle size distribution of the CNs was measured by dynamic light scattering (DLS) using a zeta potential and particle size analyzer (ELSZ-1000, Otsuka Electronics Ltd., Japan). The freeze-dried nanoparticles were observed using a field-emission scanning electron microscope (FE-SEM, Supra 55VP, Carl Zeiss, Germany) after being coated with platinum.

2.5. *In vitro* studies

2.5.1. Release test

Ten milligrams of trigger factor (TF)-loaded CNs (CNs-TF) and Mdh-loaded CNs, each suspended in 1 ml of PBS (pH 7.4) in a 1.5-ml tube, were agitated for up to 24 h at 37 °C and 220 rpm using a shaking incubator. After centrifugation (708×g, 10 min), 1 ml of supernatant was obtained at each time point, and the same amount of fresh PBS was added. The amount of released TF and Mdh protein was determined as cumulative release (wt-%) over incubation time by Pierce 660 nm protein assays kit.

2.5.2. Immunocytochemistry in THP-1 cells

Differentiated THP-1 macrophage cells (5×10^5 cells/well) were stimulated with Mdh alone (10 µg/well) and Mdh-loaded CNs (10 µg/well). Cells were fixed with 4% paraformaldehyde for 10 min at room temperature (RT) and

then permeabilized in ice-cold 0.5% Triton X-100 10 min at RT. After three washes with 0.1% PBS-T (0.1% Tween 20 in phosphate buffered saline), the samples were blocked with blocking buffer (1% bovine serum albumin in 0.1% PBS-T) for 1 h at RT, subsequently incubated with a 1:500 dilution of primary antibody (6x-His Tag mouse monoclonal antibody IgG2b, Thermo Scientific) in blocking buffer for overnight at 4 °C. After three washes with 0.1% PBS-T, cells were incubated with a 1:200 dilution of an Alexa 488-conjugated goat anti-mouse IgG2b (Invitrogen, USA) for 1 h at RT. Cells were washed in 0.1% PBS-T and mounted using Vectashield mounting medium with 4,6 diamidino-2-phenylindole (Vector Laboratory, Burlingame, CA). Images were taken 2 h, 6 h and 12 h after stimulation of Mdh and CNs-Mdh with a confocal microscopy (Zeiss LSM 800, Germany)

2.5.3. Measurement of secreted cytokines in THP-1 cells

Human leukemic monocyte cells, THP-1 cells, were stimulated as previously described [12]. Briefly, the THP-1 human leukemic monocyte cell line was cultured in RPMI 1640 medium supplemented with 10% fetal bovine serum (FBS; Gibco, USA) and antibiotic–antimycotic solution (Sigma, USA), at 37 °C under 5% CO₂. The THP-1 cells were differentiated into macrophages by stimulation with phorbol-12-myristate-13-acetate (PMA; Sigma, USA) (50 ng/ml) for 72 h, washed with FBS-free RPMI 1640 medium and incubated in 5% FBS-RPMI 1640 medium without antibiotics for 24 h before the experiments. Enzyme-linked immunosorbent assays (ELISA) were performed to evaluate cytokine secretion into the cell culture supernatant. Differentiated THP-1 macrophage cells (1×10^6

cells/well) were stimulated with recombinant proteins (10 µg/well) and protein-loaded CNs (10 µg/well for each protein). LPS (10 µg/well, Sigma, USA) and DPBS were included as positive and negative controls, respectively. The culture supernatants were collected at 6 h, 12 h and 24 h after stimulation. The amounts of tumor necrosis factor- α (TNF- α) and interleukin (IL)-6 were measured by ELISA according to the manufacturer's instructions (ThermoFisher, USA).

2.6. *In vivo* studies

2.6.1. Intranasal immunization of mice

All animal care and experimental procedures were approved by the Institutional Animal Care and Use Committee (IACUC) at Seoul National University (IACUC approval number: SNU-170504-5-3). The nasal immunization study was conducted with 6-week-old female BALB/c mice, which were divided into four groups (n = 12). The mice in each group were immunized on days 0, 14 and 28 by dropping 20 µl of PBS containing TF (30 µg)-loaded CNs, Mdh (30 µg)-loaded CNs or CNs alone into the nostrils under anesthesia. Sera, feces, and nasal and genital secretion samples were collected from each group every two weeks after the first immunization. Briefly, blood samples were obtained by cardiac puncture and were left to stand at 4 °C overnight. Sera were collected by centrifugation at 1,000×g for 10 min at 4 °C. Two or three fecal pellets were freshly collected from each mouse. PBS (10 wt-%) with protease inhibitor cocktail powder (Sigma) was added to the fecal samples, which were then vortexed and centrifuged at

16,000×g for 5 min at 4 °C. The supernatants were used for ELISAs. Nasal fluid was obtained by flushing the nasal cavity from the pharynx through the nostrils with 300 µl of PBS containing protease inhibitor cocktail. To prepare the genital secretions, the uterine horn through the vaginal region was separated, placed in 1 ml PBS containing protease inhibitor and vortexed. Centrifugation was performed at 16,000×g for 10 min at 4 °C, and the supernatants were collected. All of the prepared samples were stored at -70 °C for further analysis.

2.6.2. ELISpot assays for total IgG, IFN- γ and IL-4

Total IgG-producing B cells and IFN- γ and IL-4-secreting T cells from the spleens of 4 and 6 weeks post primary immunization (wpi) mice were measured using an Enzyme-Linked ImmunoSpot (ELISpotBasic) assay kit according to the manufacturer's instructions (Mabtech AB, Sweden). For total IgG-producing B cells, the ELISpot plates were pretreated with 70% ethanol and then to coat the plates, 100 µl of antibody solution (anti-IgG antibody; 15 µg/ml) was added and incubated overnight at 4 °C. For IFN- γ and IL-4-secreting T cells, 200 µl of monoclonal antibodies against IFN- γ (AN18, 15 µg/ml) and IL-4 (11B11, 15 µg/ml) were added to the plates and coated as described above. After incubation, the plates were washed with PBS five times and blocked with RPMI1640 containing 10% FBS for 30 min at RT. After removal of the medium, splenocytes isolated from mice at 4 and 6 wpi were added at a concentration of 1 to 2.5×10^5 cells/well. The plates were incubated at 37 °C in a humidified incubator with 5% CO₂ for 24 h for IgG or 48 h for IFN- γ and IL-4. After removing the cells, 100 µl of

biotinylated anti-IgG, IL-4, or IFN- γ antibodies in PBS containing 0.5% FBS (PBS-0.5% FBS) were added to each well. After incubation for 2 h at RT, the plates were washed and streptavidin-HRP in PBS-0.5%FBS was added and incubated for 1 h at RT. Antigen-secreting cells (ASCs) were visualized upon the addition of ready-to-use TMB substrate solution after washing the wells with PBS. The numbers of ASCs were counted using Eli.Scan+ (A.EL.VIS, Germany). These experiments were repeated three times.

2.6.3. Measurement of antibody production

Specific indirect ELISAs were performed to determine the IgG, IgG1, IgG2a and IgA titers. Briefly, using purified recombinant Mdh, each well of flat-bottom 96-well plates (Greiner Bio-One, Monroe, NC) was coated with 10 ng/well of bicarbonate buffer (pH 9.6), followed by incubation at 4 °C overnight. The plates were washed three times with PBS containing 0.05% Tween 20 (PBS-T) and were blocked at RT with 3% (w/v) BSA in PBS-T to prevent nonspecific binding. For neutralizing TF-specific antibodies, samples were pre-incubated with purified TF protein (20 μ g/well) at 37 °C for 1 h. The plates were incubated with appropriately diluted samples at RT for 2 h. The sera samples were diluted 1: 1,000 to detect specific IgG, IgG1 and IgG2a. For specific IgA measurement, the nasal wash samples were diluted 1:80, the genital secretions were diluted 1: 800, the fecal extracts were diluted 1:25 and the sera were diluted 1: 8,000. Goat anti-mouse IgG (Bio-Rad Laboratories, USA), IgG1 (Southern Biotechnology, USA), and IgG2a (Southern Biotechnology, USA) and rabbit anti-mouse IgA (BioFX

Laboratories, USA) HRP conjugates diluted 1: 2,000 (100 μ l/well) were added to the wells and incubated at RT for 1 h. Following the addition of 100 μ l of TMB as a substrate, the plates were reacted at RT for 10 min. Finally, color development was stopped by the addition of 100 μ l of 1 N H₂SO₄, and the optical density of each well was measured at 450 nm using a VersaMax microplate reader (Molecular Devices Corporation, CA, USA). Total IgA in the nasal wash, genital wash, fecal extract and serum samples was measured using a Mouse IgA ELISA Ready-SET-Go! Kit (eBioscience, San Diego, CA) according to the manufacturer's instructions.

2.7. Statistical analysis

All the data given as the mean \pm SD were analyzed by Welch's t-tests and one-way analysis of variance (ANOVA) with Tukey's post hoc multiple comparison tests using Graphpad Prism version 5 (San Diego, CA). *, P < 0.05; **, P < 0.01; and ***, P < 0.001 were considered statistically significant.

3. Results

3.1. SDS-PAGE and Western blotting

The pCold TF DNA vector is a fusion cold shock expression vector that expresses TF, an approximately 48 kDa ribosome-associated chaperone protein, as a soluble tag. The TF and Mdh proteins were characterized by SDS-PAGE and Western blot analysis. As shown in Fig. 1, the SDS-PAGE profiles indicated that purified TF and Mdh were 52.0 kDa and 85.7 kDa in size, respectively. The recombinant proteins, which were expressed from the pCold TF vector and purified using a histidine column, were confirmed by Western blotting with an anti-histidine antibody.

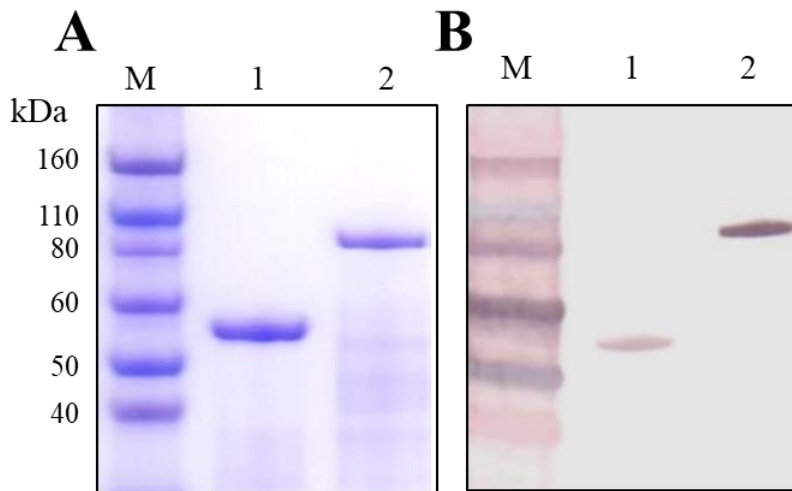


Fig. 1. (A) SDS-PAGE profiles indicated purified proteins. Lane M: Marker; Lane 1: TF and Lane 2: Mdh. TF and Mdh were 52.0 kDa and 85.7 kDa in size, respectively. (B) Western blotting of the recombinant proteins expressed from the pCold TF vector were confirmed using an anti-histidine antibody. Lane M: Marker, Lane 1: TF and Lane 2: Mdh

3.2. Characterization of recombinant protein-loaded CNs

Nanoparticle morphology was observed via scanning electron microscopy (SEM). SEM photographs showed that the CNs were spherical with a smooth-surface and uniform size (Fig. 2A). The CNs-TF and CNs-Mdh, however, were aggregated and large with bumpy surfaces compared to the CNs. The sizes of the CNs, CNs-TF and CNs-Mdh, as measured by DLS, were 324.6 ± 90.1 nm, $1,869.0 \pm 464.9$ nm and 664.6 ± 161.7 nm, respectively (Fig. 2B). As seen from the DLS results, the size distributions of all particles were uniform with a single peak.

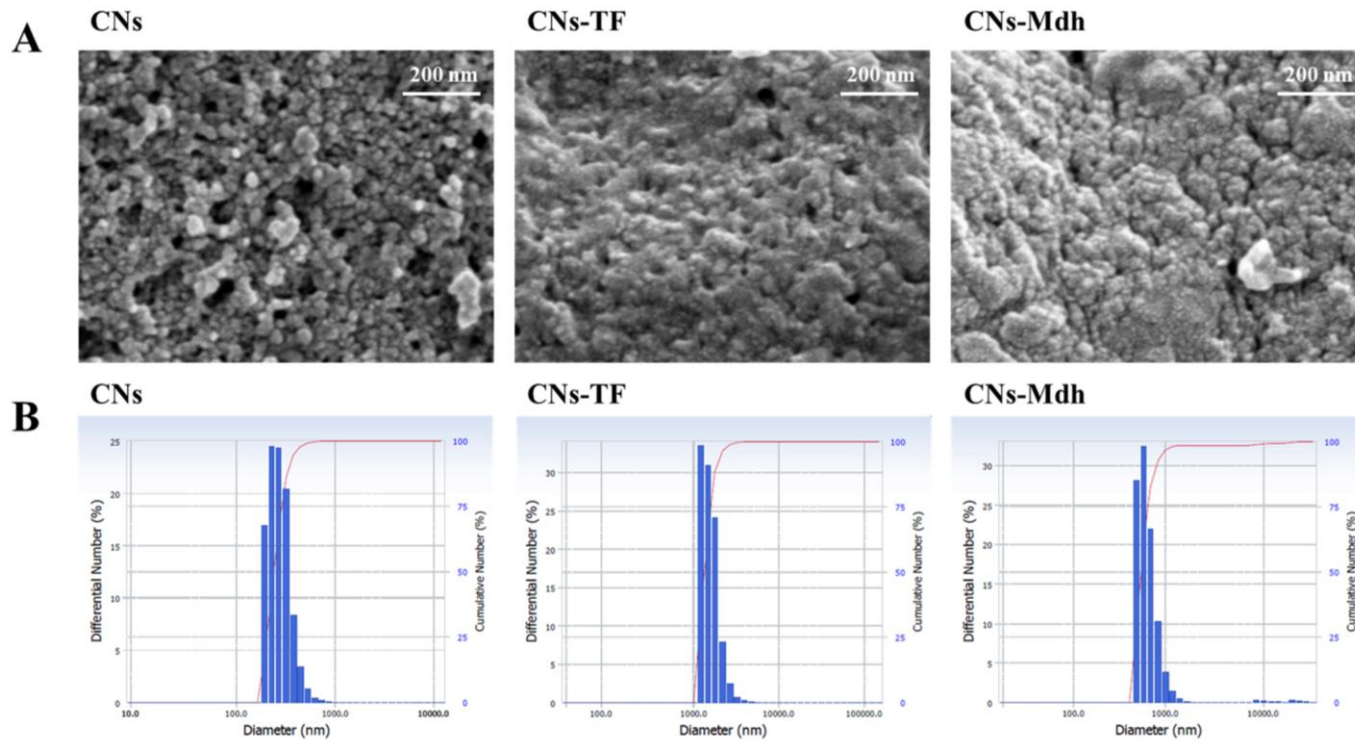


Fig. 2. (A) SEM photographs of the CNs, CNs-TF and CNs-Mdh and (B) the average particle size distribution of the CNs, CNs-TF and CNs-Mdh using dynamic light scattering (ELSZ-1000).

3.3. *In vitro* studies

3.3.1. Loading efficacy measurements and release tests for the protein-loaded CNs

The loading efficiencies of the recombinant proteins in the CNs are shown in Table 1. The loading efficiencies of TF and Mdh were $61.2\pm 3.6\%$ and $51.0\pm 0.8\%$ respectively ($n = 6$). TF showed similar loading efficiency in each tube and was approximately 10% higher than that of Mdh. Fig. 3 shows the percentage of recombinant protein released from the nanoparticles. The profile showed that 27% and 39% of TF and Mdh was released from the CNs at up to 80 h, respectively. TF and Mdh were released from the nanoparticles through a burst release within the first 24 h, which was followed by slow and steady release for next 80 h that reached a plateau.

Table 1. Loading efficiency of TF and Mdh in chitosan nanoparticles

Loaded protein	Loading efficiency (%)
TF	61.2±3.6
Mdh	51.0±0.8

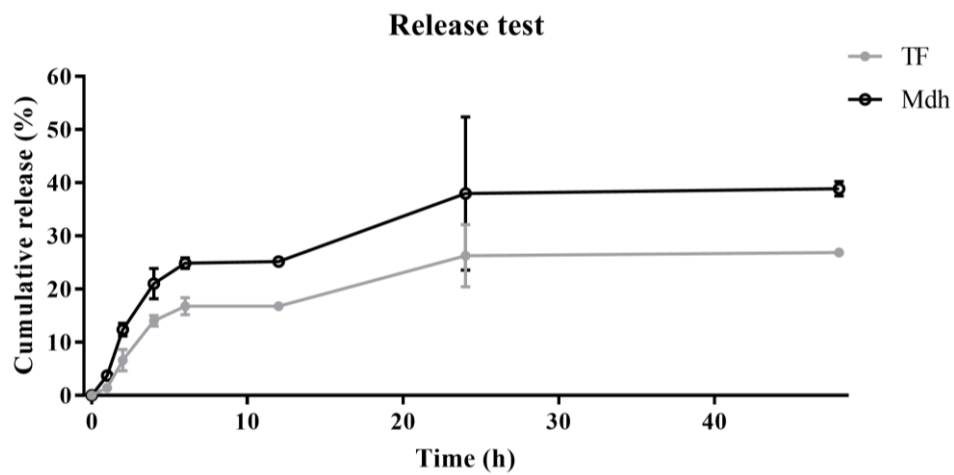


Fig. 3. Release of TF and Mdh from loaded chitosan nanoparticles.

3.3.2. Immunocytochemistry in THP-1 cells

Confocal microscopy images were taken at 2, 6, and 12 hours after stimulation with Mdh alone and CNs-Mdh in THP-1 cells (Fig. 4). The detection of the his-tagged Mdh protein was performed with anti-his antibodies and analysis via confocal fluorescence microscopy. All the images showed that the Mdh protein was localized predominantly in the nucleus in the majority of cells. In the cells stimulated with Mdh alone, the proteins were distributed in the cytosol in the first 2 hours, and the cytosolic protein intensity was faint than that in 12 hours as time passed. Similarly, when stimulated with CNs-Mdh, the Mdh protein intensity of the cytosol dimmed with time, but Mdh protein was localized predominantly in the nucleus.

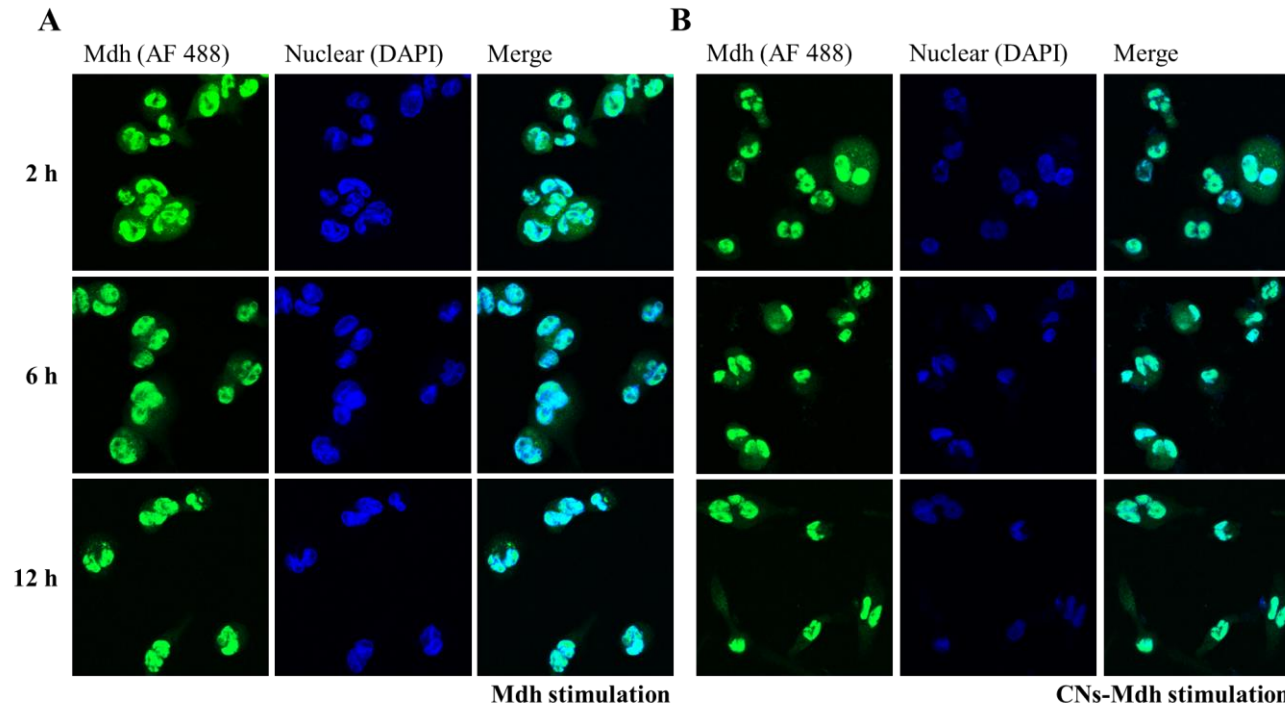


Fig. 4. Confocal microscopic analysis after immunofluorescence staining showing the nuclear localization of anti-his tag antibody conjugated with Alexa Fluor 488 (green) and nuclear staining with DAPI (blue). (A) Confocal images taken at 2 h, 6 h, and 12 h after stimulation with Mdh alone in THP-1 cells. (B) Confocal images taken at 2 h, 6 h, and 12 h after stimulation with CNS-Mdh in THP-1 cells.

3.3.3. Cytokine measurement in stimulated THP-1 cells

Culture supernatant from THP-1 cells was assayed by ELISAs for TNF- α and IL-6 after being stimulated with recombinant proteins and protein-loaded CNs (Fig. 5). The production of TNF- α decreased constantly in a time-dependent manner after antigen stimulation until 24 h. The production of IL-6 increased in a time-dependent manner after antigen stimulation until 24 h. Overall, the protein-loaded CNs-treated cells showed lower levels of TNF- α than the protein-treated cells. In the cells treated with protein alone, Mdh elicited significantly higher cytokine levels at 6 h, 12 h, and 24 h when TF and Mdh were compared; however, in the protein-loaded CNs-treated cells, the CNs-Mdh-treated cells had slightly decreased cytokine levels at 12 and 24 h compared to those of the CNs-TF-treated cells. When the TF- and Mdh-treated cells were compared, the Mdh-treated cells showed higher IL-6 secretion at all time points. The IL-6 levels were higher in the protein-treated cells than in the protein-loaded CNs-treated cells at 6 h after stimulation. However, the differences in the IL-6 levels between the protein and protein-loaded CNs-treated cells were reduced at 12 h, and the secretion of IL-6 showed a different trend at 24 h post-stimulation. The IL-6 levels in the protein-loaded CNs-treated cells exceeded those of the protein-treated cells at 24 h. In addition, the highest level of IL-6 was observed in the CNs-Mdh-treated cells, and it was a statistically significant difference when compared with that of the CNs-TF-treated cells.

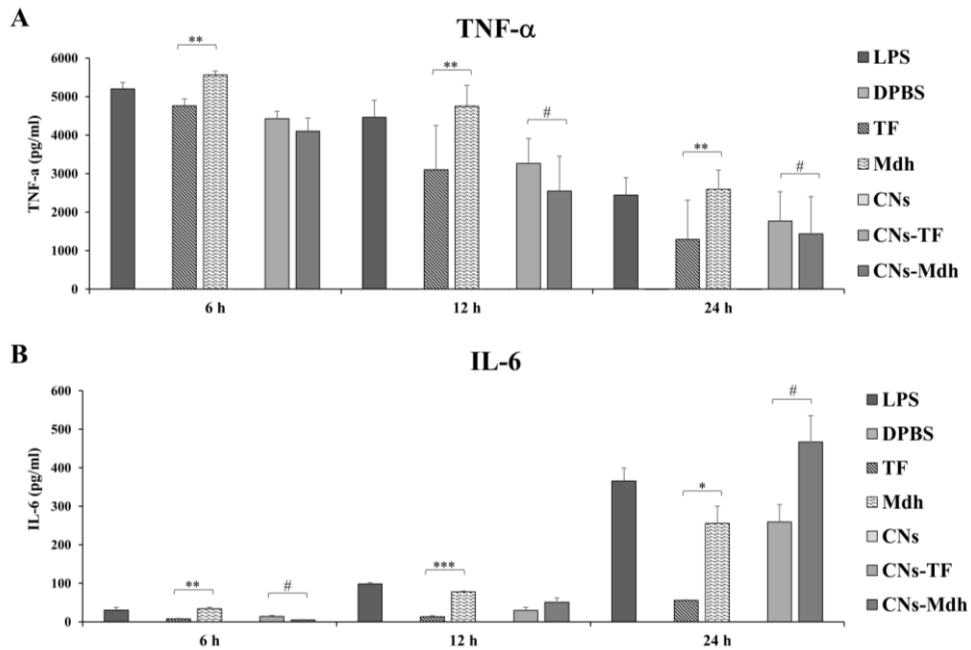


Fig. 5. TNF- α (A) and IL-6 (B) concentrations in the supernatants of THP-1 cells at 6 h, 12 h and 24 h after primary stimulation. Cells (1×10^6 cells/well) were stimulated with 10 μ g of each antigen (■: LPS, □: DPBS, ▨: TF, ▩: Mdh, □: Chitosan nanoparticles (CNs), ▨: TF loaded chitosan nanoparticles (CNs-TF), and ▩: Mdh loaded chitosan nanoparticles (CNs-Mdh)). Data are expressed the mean \pm SD, and statistical analysis was performed using Welch's t-test. * $P < 0.05$, ** $P < 0.01$, and *** $P < 0.001$ indicate significant differences between the protein-treated cells (TF and Mdh). # $P < 0.05$ indicates significant differences between the protein-loaded CNs treated cells (CNs-TF and CNs-Mdh).

3.4 *In vivo* studies

3.4.1. ELISpot

To quantify the antibody and cytokine secretory cell numbers, enzyme-linked immunosorbent (ELISpot) analysis was performed using immunized mouse splenocytes. Fig. 6 shows the average numbers of IgG, IL-4 and IFN- γ secreting cells in splenocytes at 4 and 6 wpi. At 4 wpi, the CNs-Mdh-immunized group had significantly increased numbers of IL-4 secreting cells compared to those of the PBS and CNs-immunized groups; however, there were no significant differences among the groups for of IgG and IFN- γ secreting cells. Interestingly, a different trend was observed at 6 wpi. The number of IgG-secreting B cells was significantly increased in the CNs-TF and CNs-Mdh-immunized mice compared to those of PBS and CNs-immunized mice. In addition, when the CNs-Mdh and CNs-TF-immunized groups were compared, the number of IgG-secreting cells was confirmed to be significantly increased in the CNs-Mdh-immunized mice. Unlike 4 wpi, the numbers of IL-4-secreting cells were similar in all of the groups. The number of IFN- γ -secreting cells was significantly increased in only the CNs-Mdh-immunized group compared with the PBS-immunized group.

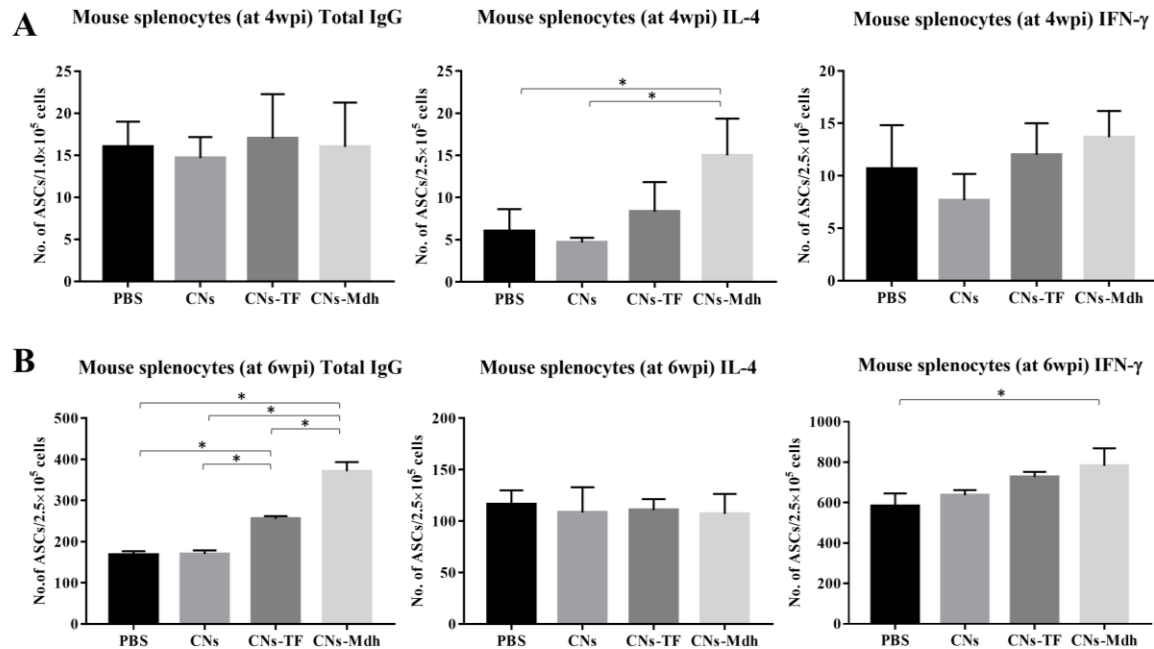


Fig. 6. ELISpot analysis in immunized mouse splenocytes. (A) The numbers of IgG, IL-4 and IFN- γ -secreting cells are shown at 4 weeks after primary immunization. (B) The numbers of IgG, IL-4 and IFN- γ -secreting cells per 2.5×10^5 cells are shown at 6 weeks after primary immunization. Values represent the mean \pm SD of three measurements per pool of splenocytes. Groups were statistically compared using one-way ANOVA with Tukey's post hoc multiple comparison test (* $P < 0.05$).

3.4.2. Measurement of Mdh specific antibodies

To study the humoral immune responses in mice induced by nasal immunization, at 6wpi, we measured the IgG, IgG1 and IgG2 levels in sera as well as IgA production in nasal washes, genital secretions, fecal extracts and sera (Fig. 7). To determine Mdh-specific antibodies, the TF-specific antibodies were neutralized, measured by ELISAs and used to determine S/N ratios (sample to negative control ratio). A slight but non-statistically significant increase in the serum IgG, IgG1 and IgG2a ELISA results, was observed for the CNs-Mdh-immunized group compared to those of the CNs-TF-immunized group. Overall, the isotype patterns of the two showed a dominance of IgG1 antibodies over IgG2a antibodies. However, Mdh-specific IgA production was elicited significantly more in serum ($P < 0.05$) and all mucosa-related samples, including nasal wash ($P < 0.001$), genital secretion ($P < 0.01$) and fecal extract ($P < 0.05$) samples, compared to the other groups.

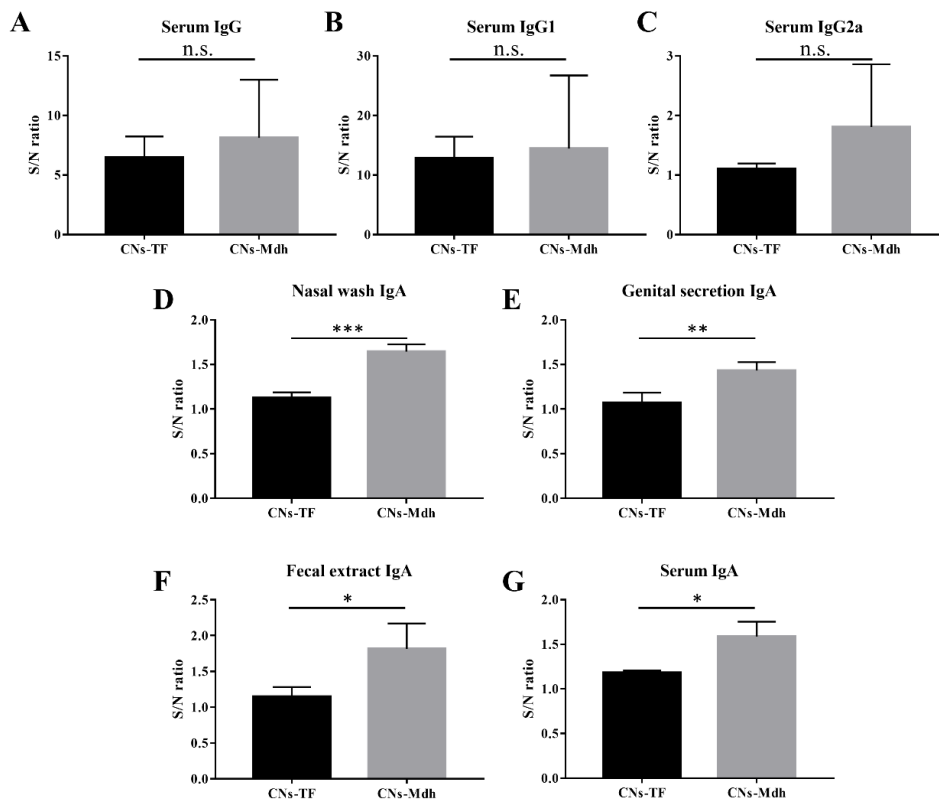


Fig. 7. Mdh-specific antibody measurements at 6 weeks after primary intranasal immunization. (A) Mdh specific total IgG, (B) IgG1 and (C) IgG2a in the sera of immunized mice. Secreted IgA and serum IgA were measured in mucosal samples and sera. Significant increase in the IgA levels of (D) nasal washes, (E) genital secretions, (F) fecal extracts and (G) sera were observed between the CNs-TF and CNs-Mdh-immunized groups. The results are expressed as the sample to negative control ratio (S/N ratio) \pm SD (n = 4), and significant differences are indicated by * $P < 0.05$, ** $P < 0.01$ and *** $P < 0.001$; n.s.; not significant CNs-TF vs CNs-Mdh).

3.4.3. Measurement of total IgA

Total IgA levels were measured for the sera, nasal washes, genital secretions and fecal extracts sampled at each period, as shown in Fig. 8 (at 2, 4 and 6 wpi). The serum IgA levels between the CNs-TF and CNs-Mdh-immunized groups were significantly different at all time points. No significant differences were observed in the nasal wash IgA levels between the CNs-TF and CNs-Mdh-immunized groups. For the genital secretions, however, a significant difference was found between the CNs-TF and CNs-Mdh-immunized groups at 2 and 6 wpi, and a very strong IgA increase in CNs-Mdh-immunized group was observed at 6wpi compared to the other groups ($P < 0.001$). Significant IgA responses were detected in the fecal extracts from the groups, with those of the CNs-Mdh-immunized group being significantly higher at 4 and 6 wpi.

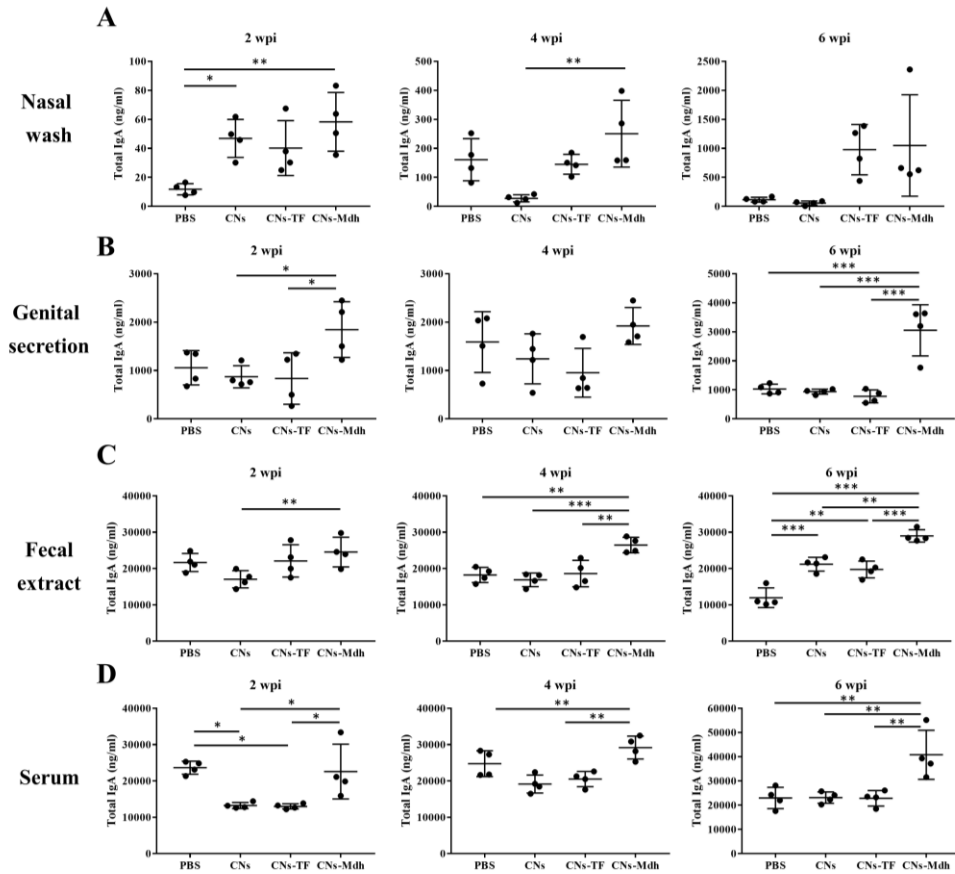


Fig. 8. Total IgA measurements in the nasal wash, genital secretion, fecal extract and serum samples at each time point (2, 4 and 6 weeks after primary immunization). Groups were statistically compared using one-way ANOVA with Tukey's post hoc multiple comparison test (* $P < 0.05$, ** $P < 0.01$, *** $P < 0.001$).

4. Discussion

As a mucosal pathogen, *B. abortus* infects humans and animals mainly through the digestive or respiratory tract. Therefore, immune induction against Brucellosis at the mucosal surface is required as the first line of defense. To induce mucosal immunity effectively and safely, candidate proteins were selected, and our group previously showed that *B. abortus* Mdh is one of the most promising candidates with effective immunostimulatory activity in THP-1 cells [12]. Mdh is a key enzyme in the TCA cycle, an important process in energy metabolism. For some intracellular organisms such as *Brucella* spp., *Toxoplasma gondii* and *Mycobacterium avium* subsp. *paratuberculosis*, partial protection and immunostimulatory effects elicited by Mdh were shown [26, 27]. Additionally, to improve mucosal immunity with an effective antigen protein, establishing an appropriate antigen delivery system for inoculation of the nasal cavity is important. For this reason, we investigated the immunological response elicited by *B. abortus* Mdh, a candidate recombinant protein, by nasal administration using CNs as an adjuvant to induce effective mucosal immunity.

In SEM photographs and DLS results, the protein-loaded nanoparticles had rougher surfaces and were approximately 2-6 times larger in size compared to the CNs alone. Since the SEM photographs were measured in a dry form, differences in size were observed with DLS, where the samples were dispersed in distilled water; the swollen form is larger than the dry form [28]. Taken together, these findings suggest that the proteins were well entrapped on the surfaces of the nanoparticles. When administered

intranasally to deliver antigen, proper particle size is critical for absorption into mucosa-associated lymphoid tissue (MALT), as many studies have demonstrated the relationship between particle size and mucociliary clearance in the airways [29, 30]. Nano- or microspheres $< 5 \mu\text{m}$ in diameter can be taken up by DCs and transferred to the spleen and lymph nodes to generate local and systemic immune responses [31]. The average size of nanoparticles in this study was less than $2 \mu\text{m}$. Therefore, we can reasonably assume that our nanoparticles are able migrate to nearby lymph nodes through phagocytosis.

In vitro release tests of TF and Mdh showed similar release profiles from the CNs that are compared to those of previous studies [20, 32, 33]. The released protein is expected to act on the nasal mucosa both in solution and in particulate form. As seen from the confocal images in THP-1 cells, Mdh released from CNs, as well as Mdh alone stimulated cells, were well penetrated into the cells. The nuclear localization of Mdh protein was observed, and the intensity of protein in cytoplasm decreased with time. It means that the CNs loaded protein is transferred well into the cell and nucleus just as it is when the protein is stimulated alone. These results indicate that CNs used as delivery vesicles do not become an obstacle when proteins are delivered into cells. TNF- α and IL-6 are major inflammatory cytokines that can be used to evaluate immune responses after antigen stimulation. THP-1 cells were differentiated into macrophages and stimulated with single proteins and protein-loaded CNs. In the cells treated with protein alone, significant differences in TNF- α and IL-6 were observed between Mdh and TF-treated cells at all time points, as has been previously reported [12]. Interestingly, unlike the protein-only stimulation, protein

loaded CNs showed different TNF- α and IL-6 secretion patterns. TNF- α was lower in the protein-loaded CNs-treated cells than in the protein-treated cells. In Caco-2 cells, chitosan nanoparticles reduce the inflammatory response induced by LPS, i.e., TNF- α inhibition, through inhibition of the NF- κ B pathway [34]. Furthermore, in RAW 264.7 macrophages, as the concentration of chitosan oligosaccharides increases, TNF- α tends to decrease, inhibiting the inflammatory effects of LPS [35]. Based on these results, the protein-loaded CNs-treated cells had decreased TNF- α production compared to protein-only stimulated cells due to the chitosan. Within the same context, TNF- α secretion in CNs-Mdh-treated cells was lower than that of CNs-TF-treated cells at 12 and 24 h because TF had a higher loading efficiency than Mdh (i.e., CNs-Mdh contained more CNs than CNs-TF). IL-6 can modulate the Th1/Th2 balance towards Th2 and was recently found to be associated with Th17 [36]. In the protein-loaded CNs-treated cells, IL-6 secretion was delayed more than in the protein-only treated cells, but it increased strongly at 24 h, at which time the IL-6 level of CNs-Mdh-treated cells was significantly higher than that of CNs-TF-treated cells. This IL-6 secretion pattern appears to be correlated with protein release from CNs. In the release test, protein was released slowly from CNs, delaying the immune response; however, an effective immune response was induced due to persistent stimulation.

For the *in vivo* studies, a significant increase in IgG-secreting cells was observed in the CNs-Mdh immunized mice (at 6 wpi), similar to Mdh-specific ELISA IgG, although there were no significant differences in the ELISA results. IL-4 secreting cells, which are involved in the Th2 immune response, were increased in the mouse splenocytes after 4 weeks of CNs-

Mdh immunization. In addition, IgG1 was more predominant than IgG2a in specific ELISAs, suggesting that CNs-Mdh induce a Th2-biased immune response. Mucosal secretions include IgA dimers and oligomers in both mice and humans. Generally, secreted IgA forms an IgA-antigen complex that binds to monocytes and macrophages through a low affinity receptor, Fc α R1 (CD89) [37]. Several cytokines associated with Th17 and Th2 immune response, including TGF- β , IL-4, IL-5, IL-6 and IL-10, stimulate secretory IgA production [38]. When IgA-opsonized particles bind to this receptor, opsonic action results, and it plays a critical role in antibody-mediated defense and the release of inflammatory mediators against infectious diseases [39], with its most important role being so-called immune exclusion, which prevents bacteria and viruses from attaching to epithelial surfaces [38]. IgA is an important component that reflects stimulation of the common mucosal immune system. In this study, specific IgA levels and total IgA levels were remarkably increased in the CNs-Mdh-immunized group compared to the CNs-TF-immunized group in all extracted samples except the total nasal wash IgA level at 6wpi. We sampled representative mucosal effector sites from the respiratory, digestive and genital mucosa and found that intranasal immunization effectively induced IgA secretion in the digestive and genital mucosa as well as in the respiratory tract of mice. When stimulated by an antigen, IgA-producing B cells are produced and then circulate in the bloodstream, eventually settling at all of the mucosal effector sites [40]. According to this mechanism, intranasally immunized CNs-Mdh seems to stimulate the development of a systemic mucosal immune response through IgA production.

5. Conclusion

Chitosan nanoparticles loaded with recombinant *B. abortus* malate dehydrogenase produced a Th2-related immune response and simultaneously increase IgA production in mice. Furthermore, the CNs-Mdh delivered through the nasal cavity induced systemic and mucosal immune responses by increasing secretory IgA in the digestive and genital mucosa as well as the nasal mucosa and by inducing serum IgA elevation. Therefore, when CNs-Mdh induce effective mucosal immunity when immunized intranasally, they comprise a promising vaccine antigen and delivery system.

6. References

1. Im, Y.B., et al., *Th2-related immune responses by the Brucella abortus cellular antigens, malate dehydrogenase, elongation factor, and arginase*. Microbial Pathogenesis, 2017. **110**: p. 7-13.
2. Yang, X., et al., *Nasal immunization with recombinant Brucella melitensis bp26 and trigger factor with cholera toxin reduces B. melitensis colonization*. Vaccine, 2007. **25**(12): p. 2261-2268.
3. Pappas, G., et al., *Brucellosis*. New England Journal of Medicine, 2005. **352**(22): p. 2325-2336.
4. Dorneles, E.M., N. Sriranganathan, and A.P. Lage, *Recent advances in Brucella abortus vaccines*. Veterinary Research, 2015. **46**(1): p. 76.
5. Oliveira, S.C. and G.A. Splitter, *Immunization of mice with recombinant L7L12 ribosomal protein confers protection against Brucella abortus infection*. Vaccine, 1996. **14**(10): p. 959-962.
6. Pasquevich, K.A., et al., *Immunization with recombinant Brucella species outer membrane protein Omp16 or Omp19 in adjuvant induces specific CD4+ and CD8+ T cells as well as systemic and oral protection against Brucella abortus infection*. Infection and Immunity, 2009. **77**(1): p. 436-445.
7. Onate, A.A., et al., *A DNA vaccine encoding Cu, Zn superoxide dismutase of Brucella abortus induces protective immunity in BALB/c mice*. Infection and Immunity, 2003. **71**(9): p. 4857-4861.
8. Hop, H.T., et al., *Immunogenicity and protective effect of*

- recombinant Brucella abortus Ndk (rNdk) against a virulent strain B. abortus 544 infection in BALB/c mice. FEMS Microbiology Letters, 2015. 362(4): p. 1-6.*
9. Simborio, H.L.T., et al., *Evaluation of the combined use of the recombinant Brucella abortus Omp10, Omp19 and Omp28 proteins for the clinical diagnosis of bovine brucellosis. Microbial Pathogenesis, 2015. 83: p. 41-46.*
 10. Lee, J.J., et al., *Proteomic analyses of the time course responses of mice infected with Brucella abortus 544 reveal immunogenic antigens. FEMS microbiology letters, 2014. 357(2): p. 164-174.*
 11. Lee, J.J., et al., *Immunoproteomic identification of immunodominant antigens independent of the time of infection in Brucella abortus 2308-challenged cattle. Veterinary Research, 2015. 46(1): p. 17.*
 12. Im, Y.B., et al., *Cytokines production and toll-like receptors expression in human leukemic monocyte cells, THP-1, stimulated with Brucella abortus cellular antigens. Microbial Pathogenesis, 2018. 122: p. 7-12.*
 13. Lowry, J.E., et al., *Vaccination with Brucella abortus recombinant in vivo-induced antigens reduces bacterial load and promotes clearance in a mouse model for infection. PLoS One, 2011. 6(3): p. e17425.*
 14. Jaganathan, K. and S.P. Vyas, *Strong systemic and mucosal immune responses to surface-modified PLGA microspheres containing recombinant hepatitis B antigen administered intranasally. Vaccine, 2006. 24(19): p. 4201-4211.*
 15. Pasquevich, K.A., et al., *An oral vaccine based on U-Omp19 induces protection against B. abortus mucosal challenge by inducing an*

- adaptive IL-17 immune response in mice*. PLoS One, 2011. **6**(1): p. e16203.
16. Neutra, M.R. and P.A. Kozlowski, *Mucosal vaccines: the promise and the challenge*. Nature Reviews Immunology, 2006. **6**(2): p. 148.
 17. Yin, L.-T., et al., *Intranasal immunisation with recombinant Toxoplasma gondii actin partly protects mice against toxoplasmosis*. PLoS One, 2013. **8**(12): p. e82765.
 18. Martin, E., et al., *Nasal mucociliary clearance as a factor in nasal drug delivery*. Advanced Drug Delivery Reviews, 1998. **29**(1-2): p. 13-38.
 19. Illum, L., et al., *Chitosan as a novel nasal delivery system for vaccines*. Advanced Drug Delivery Reviews, 2001. **51**(1-3): p. 81-96.
 20. Jiang, H.-L., et al., *In vitro study of the immune stimulating activity of an atrophic rhinitis vaccine associated to chitosan microspheres*. European Journal of Pharmaceutics and Biopharmaceutics, 2004. **58**(3): p. 471-476.
 21. Pereswetoff-Morath, L., *Microspheres as nasal drug delivery systems*. Advanced Drug Delivery Reviews, 1998. **29**(1-2): p. 185-194.
 22. Sinha, V., et al., *Chitosan microspheres as a potential carrier for drugs*. International Journal of Pharmaceutics, 2004. **274**(1-2): p. 1-33.
 23. Guliyeva, Ü., et al., *Chitosan microparticles containing plasmid DNA as potential oral gene delivery system*. European Journal of Pharmaceutics and Biopharmaceutics, 2006. **62**(1): p. 17-25.
 24. Mi, F.L., et al., *Chitosan microspheres: modification of polymeric chem-physical properties of spray-dried microspheres to control the*

- release of antibiotic drug*. Journal of Applied Polymer Science, 1999. **71**(5): p. 747-759.
25. Kang, M.L., et al., *In vivo induction of mucosal immune responses by intranasal administration of chitosan microspheres containing Bordetella bronchiseptica DNT*. European Journal of Pharmaceutics and Biopharmaceutics, 2006. **63**(2): p. 215-220.
 26. Liu, Z., et al., *Partial protective immunity against toxoplasmosis in mice elicited by recombinant Toxoplasma gondii malate dehydrogenase*. Vaccine, 2016. **34**(7): p. 989-994.
 27. Kim, W.S., et al., *A novel Th1-type T-cell immunity-biasing effect of malate dehydrogenase derived from Mycobacterium avium subspecies paratuberculosis via the activation of dendritic cells*. Cytokine, 2018. **104**: p. 14-22.
 28. Barbari, G.R., et al., *A novel nanoemulsion-based method to produce ultrasmall, water-dispersible nanoparticles from chitosan, surface modified with cell-penetrating peptide for oral delivery of proteins and peptides*. International Journal of Nanomedicine, 2017. **12**: p. 3471.
 29. Eldridge, J.H., et al., *Controlled vaccine release in the gut-associated lymphoid tissues. I. Orally administered biodegradable microspheres target the Peyer's patches*. Journal of Controlled Release, 1990. **11**(1-3): p. 205-214.
 30. Möller, W., et al., *Mucociliary and long-term particle clearance in airways of patients with immotile cilia*. Respiratory Research, 2006. **7**(1): p. 10.
 31. van der Lubben, I.M., et al., *Chitosan microparticles for oral vaccination:: preparation, characterization and preliminary in vivo*

- uptake studies in murine Peyer's patches*. *Biomaterials*, 2001. **22**(7): p. 687-694.
32. Jiang, H.L., et al., *Immune stimulating activity of an atrophic rhinitis vaccine associated to pegylated chitosan microspheres in vitro*. *Polymers for Advanced Technologies*, 2007. **18**(3): p. 220-225.
33. Kang, M.L., et al., *Pluronic® F127 enhances the effect as an adjuvant of chitosan microspheres in the intranasal delivery of Bordetella bronchiseptica antigens containing dermonecrotxin*. *Vaccine*, 2007. **25**(23): p. 4602-4610.
34. Tu, J., et al., *Chitosan nanoparticles reduce LPS-induced inflammatory reaction via inhibition of NF- κ B pathway in Caco-2 cells*. *International Journal of Biological Macromolecules*, 2016. **86**: p. 848-856.
35. Yoon, H.J., et al., *Chitosan oligosaccharide (COS) inhibits LPS-induced inflammatory effects in RAW 264.7 macrophage cells*. *Biochemical and Biophysical Research Communications*, 2007. **358**(3): p. 954-959.
36. Dienz, O. and M. Rincon, *The effects of IL-6 on CD4 T cell responses*. *Clinical Immunology*, 2009. **130**(1): p. 27-33.
37. Mkaddem, S.B., et al., *Anti-inflammatory role of the IgA Fc receptor (CD89): from autoimmunity to therapeutic perspectives*. *Autoimmunity Reviews*, 2013. **12**(6): p. 666-669.
38. Phalipon, A., et al., *Secretory Component: A New Role in Secretory IgA-Mediated Immune Exclusion In Vivo*. *Immunity*, 2002. **17**(1): p. 107-115.
39. Cerutti, A., *The regulation of IgA class switching*. *Nature Reviews Immunology*, 2008. **8**(6): p. 421.

40. Brandtzaeg, P., *The Mucosal B Cell System*, in *Mucosal Immunology (Fourth Edition)*. 2015, Elsevier. p. 623-681.

국문초록

Brucella abortus malate dehydrogenase가 담지 된 키토산 나노 입자의 비강 면역에 의한 Th2 관련 점막 면역 유도

서울대학교 대학원

수의학과 수의병인생물학 및 예방수의학 전공

소 상 희

(지도교수: 유 한 상)

본 연구에서는 *Brucella abortus*의 중요한 항원 중 하나인 malate dehydrogenase (Mdh)가 담지 된 키토산 나노입자를 BALB/c 마우스 모델에서 비강 내로 면역 후 유도되는 점막 면역 반응에 대해 조사하였다. *In vitro* 실험으로 인간 백혈병 단핵구 세포 (THP-1 세포)에서 단백질이 담지 된 키토산 나노 입자를 자극 후 사이토 카인 생성을 조사 하였다. Mdh가 담지 된 키토산 나노입자 (CNs-Mdh)로 자극 한 세포에서는 단백질로만 자극한 세포와 TF가 담지 된 키토산 나노입자 (CNs-TF)로 자극 한 세포보다 높은 interleukin(IL)-6 생산을 유도하였다. *In vivo*

실험에서는 비강 내로 면역 된 마우스에서 ELISpot을 사용하여 사이토카인 및 항체 분비 세포를 정량화하였으며, ELISA를 이용한 항체 분석을 진행하였다. ELISpot 분석 결과, CNs-Mdh 면역 군에서 면역 후 4주 및 6주 후에 각각 IL-4 및 IgG 분비 세포가 증가하는 것으로 나타났다. ELISA 결과, 면역 후 6주째에 Mdh 특이적 IgG, IgG1 및 IgG2a 항체의 증가가 확인되었으며, 특히 IgG1의 우세한 반응이 관찰되었다. 비강 내로 면역화 된 마우스의 점막 면역 반응을 분석 한 결과 CNs-TF 면역 군에 비해 CNs-Mdh 면역 군의 비강 세정액의 총 IgA를 제외하고 비강 세정액, 생식기 분비액, 분변 추출액 및 혈청에서 Mdh 특이적 IgA와 총 IgA가 유의적으로 증가 된 수치를 나타내었다. 따라서, 이러한 결과는 *B. abortus* Mdh 항원이 담지된 키토산 나노입자를 마우스의 비강 내로 면역시켰을 때, Th2 관련 면역 반응과 동시에 항원 특이적 점막 면역 반응을 효과적으로 유도한다는 것을 나타낸다.

주요어: *Brucella abortus*, malate dehydrogenase, 키토산 나노입자, Th2 면역 반응, 점막 면역 반응

학번: 2017-29538